ELSEVIER

www.elsevier.nl/locate/ica

Inorganica Chimica Acta 300–302 (2000) 769–777

Inorganica Chimica Acta

The electrochemical behaviour of electron deficient benzoheterocycle triosmium clusters

Edward Rosenberg* [a,1], Md. J. Abedin [a], Dalia Rokhsana [a], Domenico Osella* [b,2], Luciano Milone [b], Carlo Nervi [b], Jan Fiedler [c]

[a] *Department of Chemistry, University of Montana, Missoula, MT 59812, USA*
[b] *Dipartimento di Chimica IFM, Universita' di Torino, via P. Giuria 7, 10125 Turin, Italy*
[c] *J. Heyrovsky Institute of Physical Chemistry, Academy of Sciences of the Czech Republic, Dolejskova 3, 18223 Prague, Czech Republic*

Received 28 October 1999; accepted 7 December 1999

Abstract

The electrochemical behaviour of the electron deficient clusters $[Os_3(CO)_9(\mu_3\text{-}\eta^2\text{-}(L–H))(\mu\text{-}H)]$ (L = quinoline (**1**); 3-amino-quinoline (**2**); 5-amino quinoline (**3**); 6-methoxy quinoline (**4**); phenanthridine (**5**); 5,6-benzoquinoline (**6**); quinoxaline (**7**); 2-methyl benzimidazole (**8**); 2-methyl benzotriazole (**9**); 2-methyl benzothiazole (**10**); benzothiazole (**11**); 2-methyl benzoxazole (**12**)) is reported. The complexes all exhibit two one-electron electrochemically quasi-reversible reduction processes and in the case of **5** and **6** stable radical anions are formed following a one-electron reduction that is both electrochemically and chemically reversible. The electrochemical behaviour of the electron precise decacarbonyl analogues of **4**–**12** (**4′**–**12′**) was also studied in order to gain some insight into changes in the nature of the lowest unoccupied molecular orbital (LUMO) on going from the electron deficient to the electron precise cluster for a given ligand. The observed electrochemical potentials for **1**–**12** correlate with n to σ^* electronic transitions (excluding **3** and **6**) but not with the other absorptions for two series of complexes and the free ligands. The infrared spectroelectrochemistry, and ESR of $\mathbf{5}^-$ was also studied in an attempt to confirm the stability of these radical anions and to further elucidate their electronic and molecular structure.

Keywords: Electrochemistry; Osmium complexes; Heterocyclic complexes; Cluster complexes

1. Introduction

Electron deficient or coordinately unsaturated organometallic clusters have been of interest to chemists for many years [1–3]. This is due to the fact that they are generally much more reactive than their electron precise or coordinately saturated counterparts. In recent years the range of structural types which are available to the 46-electron trimetallic clusters has considerably expanded from the original examples of $[Os_3(CO)_{10}(\mu\text{-}H)_2]$ [4] and $[Fe_3(CO)_9(\mu_3\text{-}\eta^2\text{-alkyne})]$ [5]. These new examples include ruthenium bis-phosphine bridged alkyne complexes [6], heteroatom-capped clusters and molecules containing bridging phenyl ligands with three-centre two-electron bonds to two of the three metals in the cluster [7]. The common feature in all of these examples is that reaction with electron donors and electrochemical reduction invariably takes place at the metal core. Recently, we have reported the synthesis and reactivity of a class of 46-electron trimetallic clusters having a three-centre two-electron bond with a phenyl group β to a pyridinyl nitrogen contained in a fused five- or six-membered heterocyclic ring (Fig. 1) [8–12]. In the complexes studied so far we have found that with less nucleophilic two-electron donors such as amines, phosphines and methylene, nucleophilic addition is at the metal core, while with stronger nucleophiles such as hydride or carbanions nucleophilic addition is at the carbocyclic ring (Eqs. (1)–(3)) [8–12]. The latter represents a complete reversal of the nucleophilic reactivity of the uncomplexed benzoheterocycles and the ligand dependent regioselectivity is unique in the reaction chemistry of electron deficient clusters. We

[1] *Corresponding author. Tel.: +1-406-243 2592; fax: +1-406-243 4227; e-mail: rosen@selway.umt.edu
[2] *Corresponding author.

0020-1693/00/$ - see front matter
PII: S0020-1693(00)00020-7

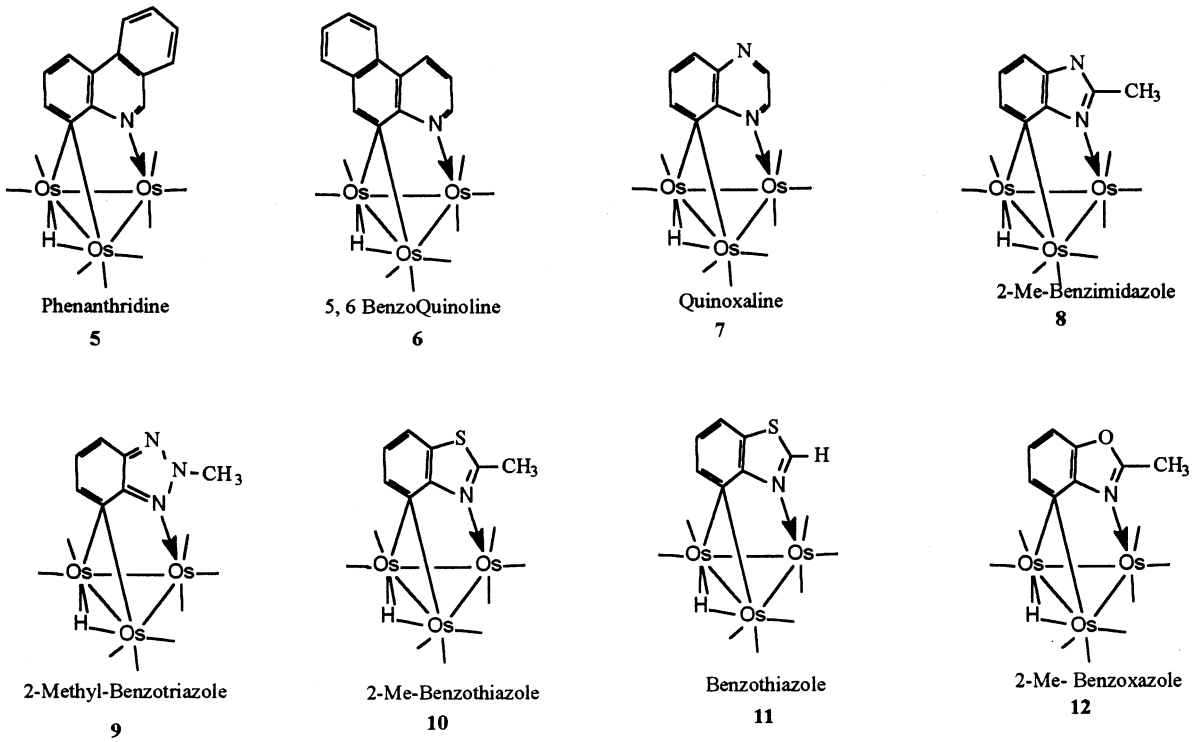

Fig. 1. Structures of the electron deficient benzoheterocycle triosmium clusters of general formula $Os_3(CO)_9(\mu_3\text{-}\eta^2(L\text{–}H))(\mu\text{-}H)$.

have already reported on the electrochemical behaviour of the quinoline complex $[Os_3(CO)_9(\mu_3\text{-}\eta^2\text{-}C_9H_6N)(\mu\text{-}H)]$ (**1**) and found that this complex undergoes the expected two-electron reduction based on the 46-electron count [8]. However, the first electron transfer at −1.38 V (Table 1), which is electrochemically reversible, is followed by a chemical reaction, which is irreversible, making the structure of this species difficult to evaluate. The value of this first reduction potential suggests that it is metal based but the subsequent chemical reaction indicates that ligand based orbitals may be involved. This is in sharp contrast to the related $[Os_3(CO)_8(\mu_3\text{-}\eta_3\text{-}Ph_2PCH_2PPh(C_6H_4))]$ and other 46-electron clusters where one-electron reduction gives a stable ESR observable radical anion [7]. The second one-electron reduction for **1** is at far more negative potential, −1.99 V (Table 1), and is irreversible.

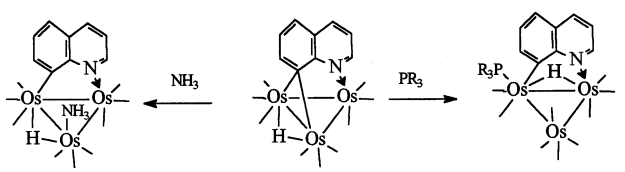

(1)

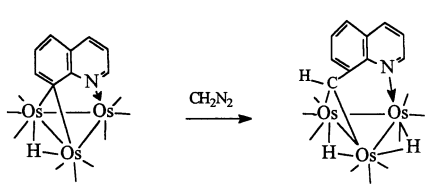

(2)

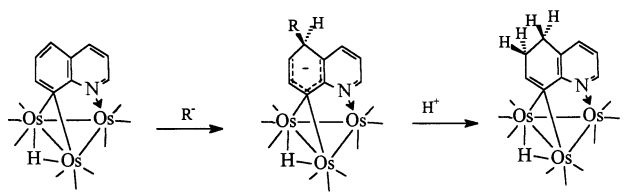

(3)

Table 1
Polarographic half-wave potentials (in volts vs. $FeCp_2/FeCp_2^+$) for electron deficient quinoline triosmium clusters $Os_3(CO)_9(\mu_3\text{-}\eta^2\text{-}C_9H_5(R)N)(\mu\text{-}H)$ [a]

Compd	R	Oxidation	Reductions	Solvent
1	H	$+0.14(E_{IRR})$	$-1.38(E_{REV}C)$, $-1.99(E_{IRR})$	CH_2Cl_2
		$+0.07(E_{IRR})$	$-1.26(E_{REV}C)$, $-2.02(E_{IRR})$	CH_3CN
2	3-NH_2	$+0.17(E_{IRR})$	$-1.37(E_{REV}C)$, $-1.92(E_{IRR})$	CH_2Cl_2
3	5-NH_2	$+0.15(E_{IRR})$	$-1.49(E_{REV}C)$, $-2.02(E_{IRR})$	CH_2Cl_2
		$-0.06(E_{IRR})$	$-1.37(E_{REV}C)$, $-1.99(E_{IRR})$	CH_3CN
4	6-OCH_3	$+0.20(E_{IRR})$	$-1.34(E_{REV}C)$, $-1.89(E_{IRR})$	CH_2Cl_2

[a] E_{REV} = reversible, E_{IRR} = irreversible, C = chemical reaction following reduction.

Table 2
Polarographic half-wave potentials (in volts vs. $FeCp_2/FeCp_2^+$) for electron precise quinoline triosmium clusters $Os_3(CO)_{10}(\mu_3\text{-}\eta^2\text{-}C_9H_5(R)N)(\mu\text{-}H)$ [a]

Compd	R	Oxidation	Reduction	Solvent
1′	H	$+0.24(E_{IRR})$	$-2.01(E_{IRR}, 2e^-)$	CH_2Cl_2
2′	3-NH_2	$+0.16(E_{IRR})$	$-2.03(E_{IRR}, 2e^-)$	CH_2Cl_2
4′	6-OCH_3	$+0.25(E_{IRR})$	$-2.07(E_{IRR}, 2e^-)$	CH_2Cl_2

[a] E_{REV} = reversible, E_{IRR} = irreversible, C = chemical reaction following reduction.

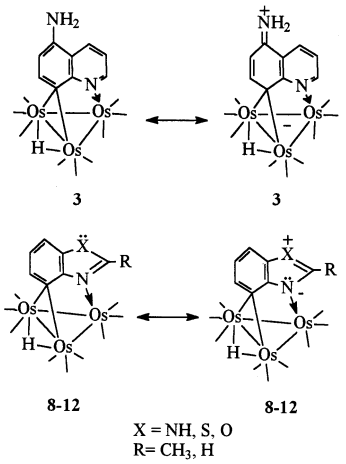

Scheme 1. Contributing resonance forms for **3** and **8**–**12**.

Table 3
UV–Vis data for electron deficient quinoline triosmium clusters $Os_3(CO)_9(\mu_3\text{-}\eta^2\text{-}C_9H_5(R)N)(\mu\text{-}H)$ [a,b]

Compd	R	n–σ^*	MLCT	π–π^*
1	H	662	369	316
2	3-NH_2	647	367	317
3	5-NH_2	598	401	321
4	6-OCH_3	655	374	316

[a] In nanometers.
[b] In methylene chloride.

The electrochemical behaviour of **1** suggests that the second electron transfer is ligand based and that ligand cleavage is probably involved [8]. Given that electrochemical studies have yielded useful information about the electronic structure of electron deficient trimetallic clusters, the large variation in ligand structure represented by the series $[Os_3(CO)_9(\mu_3\text{-}\eta^2\text{-}(L\text{–}H))(\mu\text{-}H)]$ (L = quinoline (**1**); 3-amino-quinoline (**2**); 5-amino quinoline (**3**); 6-methoxy quinoline (**4**); phenanthridine (**5**); 5,6-benzoquinoline (**6**); quinoxaline (**7**); 2-methyl benzimidazole (**8**); 2-methyl benzotriazole (**9**); 2-methyl benzothiazole (**10**); benzothiazole (**11**); 2-methyl benzoxazole (**12**)), and the somewhat ambiguous results obtained from our initial studies of **1**, we thought it would be useful to make a full electrochemical study of this series of metal clusters. We report here the results of these studies as well as our attempts to further characterise the reduced species and to correlate their electrochemical behaviour with their spectroscopic and chemical properties.

2. Results and discussion

The polarographic half-wave potentials for the monosubstituted complexes **2**–**4** are given in Table 1. As expected, the first one-electron reduction occurs at much less negative potentials than their electron precise dodecacarbonyl analogues, **2′**–**4′** (Table 2). This first reduction potential is relatively insensitive to substitution on the quinoline ring except in the case of the 5-amino derivative, **3**, where about a 0.1 V shift to more negative potential is observed. This is consistent with the observations that **3** is more basic towards protonation and is much less reactive towards two electron donors than the other the monosubstituted quinolines examined to date [9]. The apparently greater electron density at the metal core is most likely due to the contribution of a resonance structure in which the lone pair on nitrogen transfers electron density to the metal core (Scheme 1). The UV–Vis spectrum of **3** is also significantly different than **1**, **2** and **4** (Table 3). The band in the 600 nm region, assigned to the n–σ^* transition of the metal core, is shifted to shorter wavelength, while the band in the 350–400 nm region, assigned to the metal to ligand charge transfer band is shifted to shorter wavelength. If more electron density is transferred to metal–metal bonding MOs an increase in the energy of the σ^* orbitals would be expected and a secondary increase in the energy of the non-bonding metal MOs would also result. This would increase the energy of the n–σ^* transition and decrease the energy of the metal to ligand charge transfer band, as observed. The assignments of these bands as given here are based on generally accepted assignments for metal carbonyl clusters [13], but the close proximity of the MLCT and the π–π^* transitions makes these two assignments interchangeable in some cases.

On the other hand, the magnitude of the change in the first reduction potential of **3** relative to **1**, **2** an **4** does not seem large enough to account for the great difference in reactivity observed and thus the reduction potentials measured for **3** may reflect a more complex situation. This is suggested by the behaviour of **1**–**4** immediately after the first one-electron reduction that was studied in detail for **3**. In acetonitrile, which provides a wider potential window, two one-electron reduction waves are observed for **3** on a dropping

mercury electrode (DME) at $E_{1/2}(0/-1) = -1.37$ V and $E_{1/2}(-1/-2) = -1.99$ V versus Fc/Fc^+. A third reduction process, probably corresponding to a ligand centred reduction, appears at $E_{1/2}(-2/-3) = -2.76$ V. Polarographic logarithmic analysis indicates the Nernstian behaviour of the first reduction process while the second process appears to be slightly irreversible. The one-electron consumption of the $(0/-1)$ reduction was confirmed by controlled potential coulometry. The $(0/-1)$ reduction process is followed by a fast chemical reaction of unknown origin. Analysis of the AC polarographic data provides the rate constant of this chemical reaction, $k = 760\ s^{-1}$. It is this rapid reaction at the electrode that probably mitigates the value of the first reduction potential for **3**.

The phenanthridine and 5,6-benzoquinoline complexes **5** and **6** reduced in two one-electron steps in CH_2Cl_2 and acetonitrile solutions with almost identical values (Table 4). Surprisingly, no chemical reaction complicates the first Nernstian electron transfer and a long-lived monoanion $\mathbf{5}^-$ can be obtained by exhaustive controlled-potential electrolysis (made on a Hg-pool electrode). No EPR signal could be detected in the electrolysed solution even at liquid nitrogen temperature. This may be due to a very short relaxation time for the unpaired electron in $\mathbf{5}^-$, which is certainly stable on the overall time-scale of the experiment (see below). The second reduction for both **5** and **6** appears to be irreversible with the voltammetric reoxidation peak positioned about 0.8 V positively from the cathodic reduction peak. In acetonitrile, a third reversible reduction can be observed at a potential very close to that of the free ligand (Fig. 2), but this probably does not involve the cleaved ligand. This behaviour is very similar to that of **1** and **3**.

Spectroelectrochemistry performed in an OTTLE [14] infrared cell in the case of **5** shows that during the reduction two isosbestic points can be located in the CO stretching region of the infrared spectrum at 2015 and 1965 cm^{-1}. Reoxidation completely restores the original spectrum of the neutral compound, confirming the complete stability of the cluster anion, $\mathbf{5}^-$ (Fig. 3). The infrared spectrum and the reversibility of the reduction suggest a radical anion that is very similar in structure to **5**. Recently, stable radical anions derived from the 48-electron clusters $[Os_3(CO)_9(H)L]$ (L = ortometalated diimine) have been identified [15]. These results clearly demonstrate that the additional delocalization available to the tricyclic aromatic ligands has a strong influence on the stability of the product formed after the first one-electron electron reduction, and lends support to the suggestion made earlier in this report that this step is not strictly metal based. The free ligand undergoes an irreversible two-electron reduction at -2.46 V in acetonitrile, and this value is very similar to that observed for the third one-electron reduction in **5**. We can speculate that coordination to the metal fragment makes the reduction of the ligand split into two separate one-electron steps, only the first of which is detectable in the actual potential window. However, the latter is reversible and therefor suggests that the ligand is still bound to the cluster. There are only small

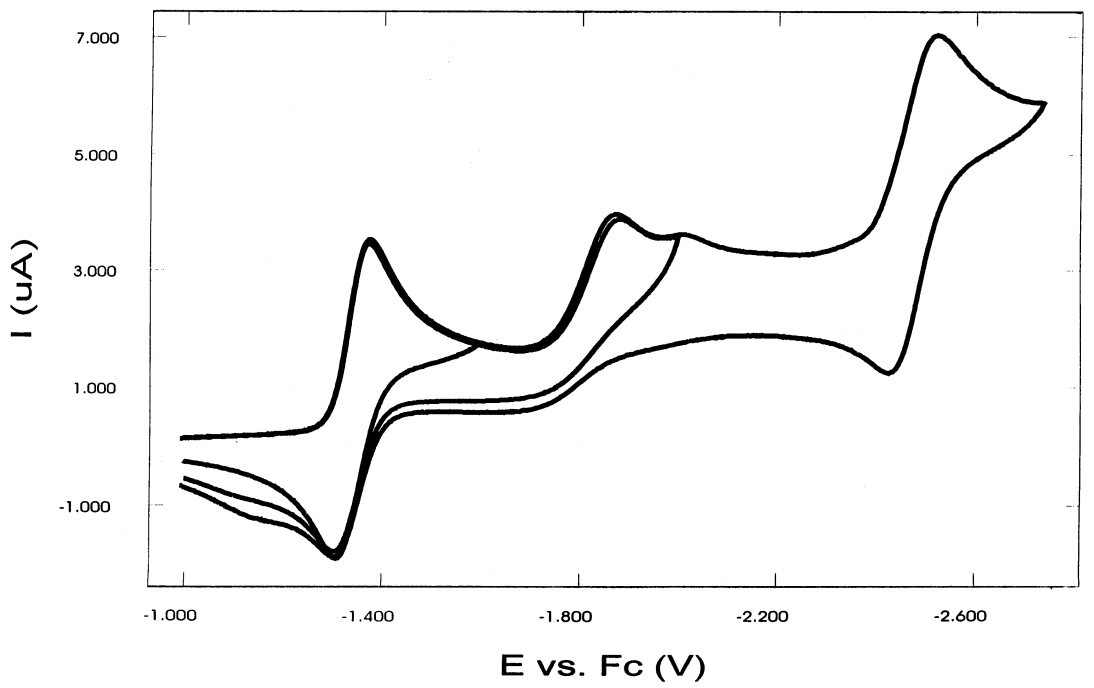

Fig. 2. CV response of an acetonitrile solution of **5** on a glassy carbon electrode at 200 mV s^{-1} showing the three one-electron reductions and the reversibility of the first half-wave potential.

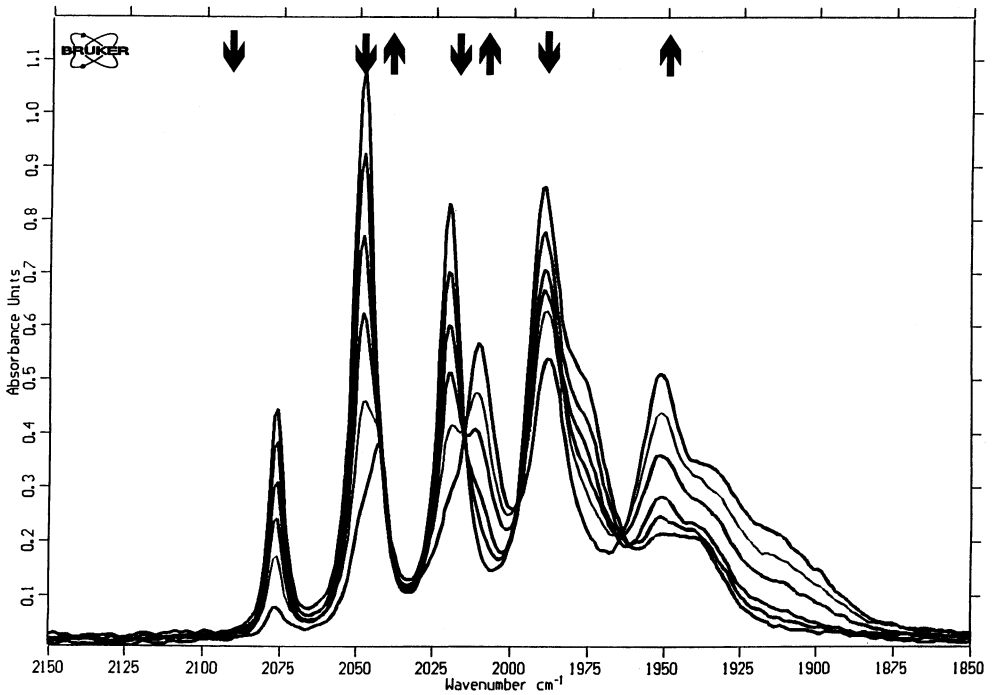

Fig. 3. Time resolved infrared spectroelectrochemical response of a CH_2Cl_2 solution of **5** in the carbonyl stretching region recorded in the OTTLE cell scanning potentials from -1.40 to -1.65 V vs. Fc/Fc^+ (scan rate = 5 mV s^{-1}) and showing the conversion of **5** to $\mathbf{5}^-$ with added current.

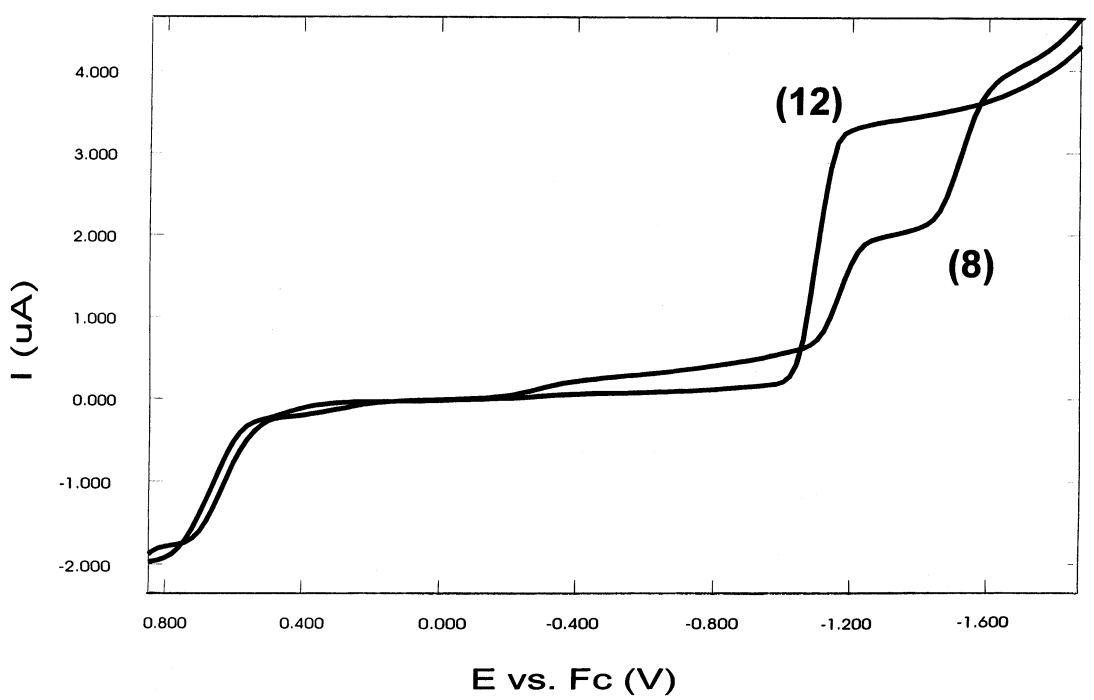

Fig. 4. Controlled potential coulometry of **8** and **12** showing the two-electron current for **12** and the one-electron for **8**.

differences in the electronic absorption spectra of **5** and **6** relative to **1**, **2** and **4** and in fact the values of the 0/1-reduction potentials are similar (vide infra).

Derivatives (**7**–**9**) behave similarly to **1**–**6** and have been studied in CH_2Cl_2 and THF solutions. Acetonitrile could not be used as a solvent because unlike **1**–**6** these complexes form adducts with acetonitrile at room temperature [16]. For compounds **7** and **9** the second one-electron reduction process is shifted towards very negative potentials and can only be observed in THF; solvent discharge making them unobservable in CH_2Cl_2. Complex **8**, on the other hand, has its first

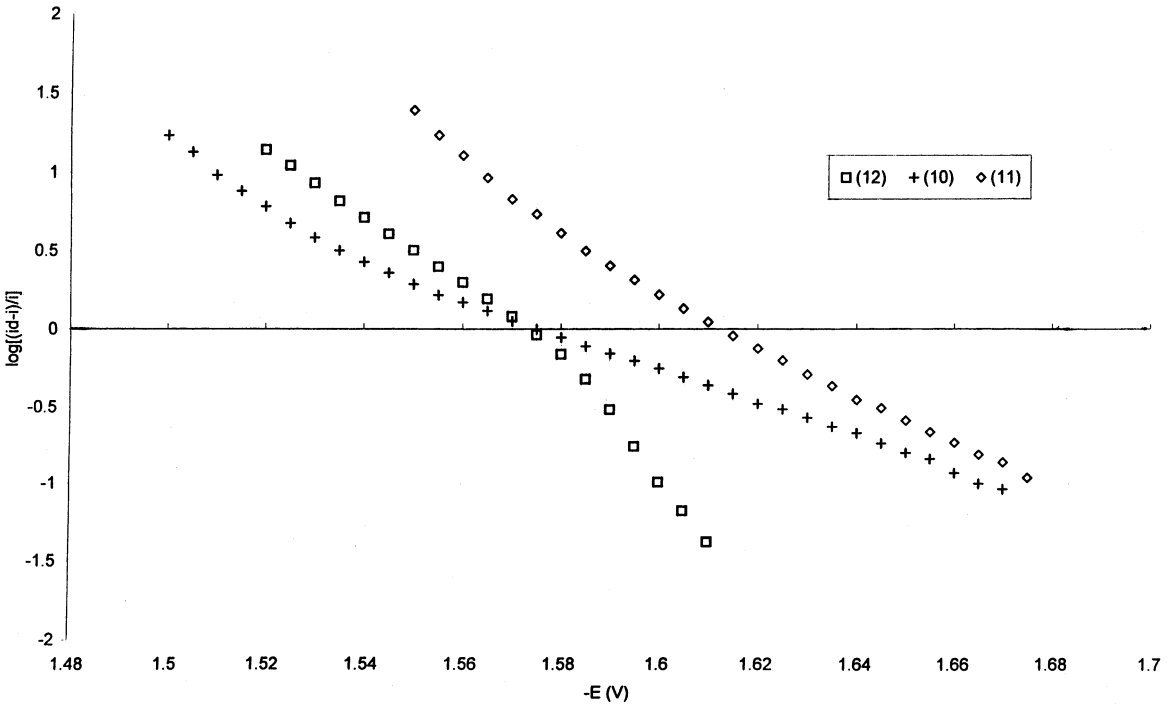

Fig. 5. Polarographic logarithmic analysis of **10**–**12** showing the non-linearity associated with two overlapping one-electron transfers.

one-electron reduction shifted to slightly more negative potentials with its second reduction being very similar to **1**–**6**. This shift may be due to contributions from resonance structures involving the pyrrole nitrogen that places additional negative charge on the metal core (Scheme 1).

Complexes **10**–**12** show different responses from those described above. In CH_2Cl_2 solution on a DME a single two-electron reduction wave is observed, which is twice the height of the waves observed for the one-electron wave of structurally analogous cluster **8** at the same concentration (Fig. 4).

Nevertheless polarographic logarithmic analysis of the two-electron waves of **10**–**12** result in non-linear plots, which indicate that waves are composed of two overlapping one-electron steps (Fig. 5) as is the case for

Table 4
Polarographic half-wave potentials (in volts vs. $FeCp_2/FeCp_2^+$) for electron deficient benzoheterocycle triosmium clusters $Os_3(CO)_9(\mu_3\text{-}\eta^2\text{-}(L\text{–}H))(\mu\text{-}H)$ [a]

Compd	L	Oxidation	Reduction	Solvent
5	Phenanthridine	$+0.20(E_{IRR})$	$-1.52(E_{REV})$, $-1.84(E_{IRR})$	CH_2Cl_2
		$+0.00(E_{IRR})$	$-1.34(E_{REV})$, $-1.68(E_{IRR})$, $-2.45(E_{REV})$	CH_3CN
6	5,6-Benzoquinoline	$+0.22(E_{IRR})$	$-1.44(E_{REV})$, $-1.78(E_{IRR})$	CH_2Cl_2
			$1.33(E_{REV})$, $-1.78(E_{IRR})$, $-2.56(E_{REV})$	CH_3CN
7	Quinoxaline	$+0.23(E_{IRR})$	$-1.16(E_{REV}C)$	CH_2Cl_2
		$+0.12(E_{IRR})$	$-1.05(E_{REV}C)$, $-2.41(E_{IRR})$, $-2.60(E_{QREV})$	THF
8	2-Methyl benzimidazole	$+0.15(E_{IRR})$	$-1.64(E_{REV}C)$, $-1.99(E_{IRR})$	CH_2Cl_2
9	2-Methyl benzotriazole	$+0.19(E_{IRR})$	$-1.37(E_{REV}C)$	CH_2Cl_2
		$+0.09(E_{IRR})$	$-1.26(E_{REV}C)$, $-2.61(E_{IRR})$, $-2.92(E_{QREV})$	THF
10	2-Methyl benzothiazole	$+0.24(E_{IRR})$	$-1.62(E_{IRR}, 2e^-)$	CH_2Cl_2
11	Benzothiazole	$+0.16(E_{IRR})$	$-1.57(E_{QREV}, 2e^-)$	CH_2Cl_2
12	2-Methyl benzoxazole	$+0.21(E_{IRR})$	$-1.56(E_{QREV}, 2e^-)$	CH_2Cl_2

[a] E_{REV} = reversible, E_{QREV} = quasi-reversible, E_{IRR} = irreversible, C = chemical reaction following reduction.

almost all two electron processes. Significantly, the electron precise analogues of these complexes, **9′**–**12′**, undergo similar two-electron (or more likely, two overlapping one-electron steps) reductions but shifted to more negative potentials. This suggests that the LUMOs in this series of complexes are primarily ligand in character and that the impact of the formal electron deficiency at the metal core is to lower the energy of the LUMO with a corresponding decrease in the energy of the HOMO. However, as for **8**, a shift towards more negative potential is observed for the initial electron transfer, which can be rationalised by contributions from resonance structures involving the second heteroatom, which places some additional electron density at the metals (Scheme 1). This shift is not observed in **9** where such resonance structures are not accessible.

In conclusion, the variation of ligands results in much larger variation of the second-reduction potential (in CH_2Cl_2 from -1.56 to -2.61 V) when compared to the first-reduction process, the electrode potential of which is appreciably modified by the heterocycle (from -1.16 to -1.64 V). Very interesting is the difference between the first and second reduction potentials, which varies over a large range from approximately 0.0 to 1.36 V. This observation corroborates the hypothesis that the second electron transfer involves a molecular orbital with larger contributions from the heterocyclic ligand. As expected, the electron precise clusters are all reduced at more negative potentials much closer to the free ligands (-2.40 to -2.50 V) and significantly, over a much narrower range (-1.93 to -2.07 V, Table 5) than their electron deficient counterparts. The one exception to this trend is **7′**, which shows a fully reversible one-electron reduction at much less negative potential (-1.63 V). The free ligand, quinoxaline is also reduced at less negative potential by a multielectron process. (-2.18 V). These overall trends are also seen in the electronic spectra where the metal to ligand charge transfer bands are relatively insensitive to changes in the heterocycle except for **7′**, which shows a band at much longer wavelengths, 486 nm (Tables 6–8). In the case of the electron deficient complexes a reasonable correlation ($R^2 = 0.90$) is observed between the n to σ^* transition and the first reduction potential, if one excludes compounds **3** and **6** where the five-position of the quinoline ring is occupied (Fig. 6). Inclusion of these compounds significantly degrades the correlation. No other correlations between the UV–Vis data and the electrochemical data were found. This correlation and all of the other data discussed above leads to the conclusion that the first reduction potential is primarily metal based but is appreciably modified by the heterocycle and in particular for the quinoline series when substituted in the five-position. A more quantitative

Table 6
UV–Vis data for electron precise quinoline triosmium clusters $Os_3(CO)_{10}(\mu_3\text{-}\eta^2\text{-}C_9H_5(R)N)(\mu\text{-}H)$ [a,b]

Compd	R	MLCT	π–π*
1′	H	384	350
2′	3-NH_2	396	358
4′	6-OCH_3	390	351

[a] In nanometers.
[b] In methylene chloride.

Table 7
UV–Vis data for electron deficient quinoline triosmium clusters $Os_3(CO)_9(\mu_3\text{-}\eta^2\text{-}C_9H_5(R)N)(\mu\text{-}H)$ [a,b]

Compd	L	n–σ*	MLCT	π–π*
5	Phenanthridine	637	380	340
6	5,6-Benzoquinoline	610	370	340
7	Quinoxaline	720	370	310
8	2-Methyl benzimidazole	607	362	345 sh
9	2-Methyl benzotriazole	670	358	268
10	2-Methyl benzothiazole	609	351	268
11	Benzothiazole	630	350	270
12	2-Methyl benzoxazole	605	355	260

[a] In nanometers.
[b] In methylene chloride.

Table 5
Polarographic half-wave potentials (in volts vs. $FeCp_2/FeCp_2^+$) for electron precise benzoheterocycle triosmium clusters $Os_3(CO)_{10}(\mu_3\text{-}\eta^2\text{-}(L\text{–}H))(\mu\text{-}H)$ [a]

Compd	L	Oxidation	Reduction	Solvent
5′	Phenanthridine	$+0.21(E_{IRR})$	$-1.96(E_{IRR}, 2e^-)$	CH_2Cl_2
6′	5,6-Benzoquinoline	$+0.24(E_{IRR})$	$-1.98(E_{IRR}, 2e^-)$	CH_2Cl_2
7′	Quinoxaline	$+0.27(E_{IRR})$	$-1.63(E_{REV}, 2e^-)$	CH_2Cl_2
8′	2-Methyl benzimidazole	$+0.18(E_{IRR})$	$-2.22(E_{IRR}, 2e^-)$	CH_2Cl_2
9′	2-Methyl benzotriazole	$+0.29(E_{IRR})$	$-1.92(E_{IRR}, 2e^-)$	CH_2Cl_2
10′	2-Methyl benzothiazole	$+0.30(E_{IRR})$	$-1.93(E_{IRR}, 2e^-)$	CH_2Cl_2
11′	Benzothiazole	$+0.25(E_{IRR})$	$-2.07(E_{IRR}, 2e^-)$	CH_2Cl_2
12′	2-Methyl benzoxazole	$+0.27(E_{IRR})$	$-2.05(E_{IRR}, 2e^-)$	CH_2Cl_2

[a] E_{REV} = reversible, E_{QREV} = quasi-reversible, E_{IRR} = irreversible, C = chemical reaction following reduction.

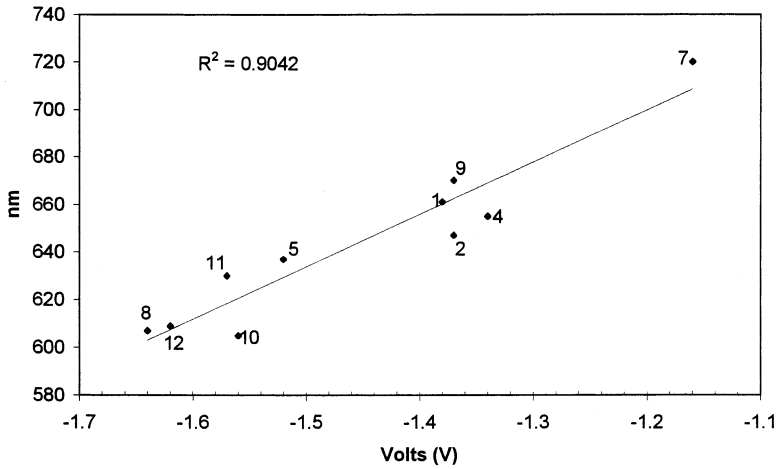

Fig. 6. Plot of the *n* to σ* transition (605–720 nm region) vs. the first one-electron reduction potential for the electron deficient complexes, $Os_3(CO)_{10}(\mu_3\text{-}\eta^2\text{-(L–H)})(\mu\text{-H})$ not including **3** and **6**.

Table 8
UV–Vis data for electron precise quinoline triosmium clusters $Os_3(CO)_{10}(\mu_3\text{-}\eta^2\text{-(L–H)})(\mu\text{-H})$ [a,b]

Compd	L	MLCT	π–π*
5′	Phenanthridine	396, 377 sh	320 sh
6′	5,6-Benzoquinoline	382	277
7′	Quinoxaline	486,381	300
8′	2-Methyl benzimidazole	393	322
9′	2-Methyl benzotriazole	400	281
10′	2-Methyl benzothiazole	400	300
11′	Benzothiazole	389	275 sh
12′	2-Methyl benzoxazole	[c]	[c]

[a] In nanometers.
[b] In methylene chloride.
[c] Too unstable with respect to conversion to **12** to obtain data.

assessment of these effects will be forthcoming from Fenske–Hall molecular orbital calculations and from the continued study of the reactivity of these complexes, both of which are currently underway in our laboratories.

3. Experimental

Compounds **1**–**12** were synthesised by known literature procedures [8–12]. Solvents were distilled from conventional drying agents before use (dichloromethane and acetonitrile, calcium hydride; tetrahydrofuran, benzophenone ketyl). Voltammetric and polarographic measurements were performed with a PAR 273 electrochemical analyser interfaced to a PC. A three electrode cell was designed to allow the tip of the standard calomel electrode (SCE) to be as close as possible to the working electrode. Compensation for the *IR* drop was applied through a positive feedback loop. All measurements were carried out under argon using anhydrous deoxygenated solvents. Solutions were 10^{-3} M for the compounds under investigation and 10^{-1} M for the supporting electrolyte, $[N^nBu_4][PF_6]$. The working electrodes used were: a hanging mercury drop electrode (HMDE), a dropping mercury electrode (DME); or a glassy carbon electrode (GCE). Potential data (versus SCE) are referred to the ferrocene $(0/+1)$ couple; under our experimental conditions the ferrocene/ferrocenium ion couple is located at $+0.46$ V in methylene chloride, at $+0.40$ V versus SCE in acetonitrile and at $+0.45$ V in tetrahydrofuran. Infrared spectroelectrochemistry was performed in an OTTLE cell built using the design of Krejcik et al. [14]. UV–Vis spectra were obtained on a Perkin–Elmer Lambda 11or a Kontron Uvikon 930 spectrophotometer. NMR spectra were obtained on a Jeol EX–400 or a Varian Unity Plus spectrometer.

Acknowledgements

We gratefully acknowledge the National Science Foundation (grant no. 9625367, E. Rosenberg), the Consiglio Nazionale delle Ricerche (CNR L. Milone), the NATO Science Program (grant no. CRG971416, E. Rosenberg and L. Milone) and MURST (COFIN 98/99).

References

[1] R.D. Adams, F.A. Adams (Eds.), Catalysis by Di- and Polynuclear Metal Cluster Complexes, Wiley–VCH, New York, 1998 (Chapter 2).

[2] R.D. Adams, H.D. Kaesz, D.F. Shriver (Eds.), The Chemistry of Transtion Metal Cluster Complexes, VCH, New York, 1991 (Chapter 4).
[3] B.F.G. Johnson, R.E. Benfield, in: B.F.G. Johnson (Ed.), Transition Metal Clusters, Wiley, Chichester, 1980 (Chapter. 4).
[4] J. Keister, J.R. Shapley, Inorg. Chem. 21 (1982) 3304.
[5] W.A. Olson, A.M. Stacy, L.F. Dahl, J. Am. Chem. Soc. 108 (1986) 7646.
[6] G. Lavigne, B. de Bonneral, in: R.D. Adams, F.A. Cotton (Eds.), Catalysis by Di- and Polynuclear Metal Cluster Complexes, Wiley–VCH, New York, 1998, p. 54.
[7] M.P. Brown, P.A. Dolby, M.M. Harding, A.J. Mathews, A.K. Smith, D. Osella, M. Abrun, R. Gobetto, J. Chem. Soc., Dalton Trans. (1993) 827.
[8] E. Arcia, D.S. Kolwaite, E. Rosenberg, K. Hardcastle, J. Ciurash, R. Duque, R. Gobetto, L. Milone, D. Osella, M. Botta, W. Dastru', A. Viale, J. Fiedler, Organometallics 17 (1998) 415.
[9] A. Bar Din, B. Bergman, E Rosenberg, R. Smith, W. Dastru', R. Gobetto, L. Milone, A. Vialle, Polyhedron 17 (1998) 3168.
[10] B. Bergman, R. Holmquist, R. Smith, E. Rosenberg, K.I. Hardcastle, M. Visi, J. Ciurash, J. Am. Chem. Soc. 120 (1998) 12818.
[11] R. Smith, E. Rosenberg, K.I. Hardcastle, V. Vazquez, J. Roh, Organometallics 18 (1999) 3519.
[12] Md.J. Abedin, B. Bergman, R. Holmquist, R. Smith, E. Rosenberg, J. Ciurash, K.I. Hardcastle, J. Roe, V. Vazquez, C. Roe, S.E. Kabir, B. Roy, S. Alam, K.A. Azam, Coord. Chem. Rev. 190–2 (1999) 975.
[13] H. Knozinger, in: B.C. Gates, L. Guczi, H. Knozinger (Eds.), Metal Clusters in Catalysis, Elsevier, Amsterdam, 1986, p. 173.
[14] M. Krejcik, M. Danik, F. Hartl, J. Electroanal. Chem. 317 (1991) 179.
[15] J. Nijhoff, F. Hartl, J.W.M. van Outersterp, D.J. Stufkens, M.J. Calhorda, L.F. Veiros, J. Organomet. Chem. 573 (1999) 121.
[16] E. Rosenberg, Md.J. Abedin, D. Rokhsana, L. Milone, R. Gobetto, A. Viale, W. Dastru', in preparation.